Accurate Design, Calculation and Analysis of Two Square Power Pads for Stationery Wireless Power Transfer in Electric Vehicle

Dilip R Dobariya[a]*, Hina Chandwani[b]

[a] *Research Scholar,The Maharaja Sayajirao University of Baroda Vadodara, India.*
[b] *Associate Professor(Retd.),The Maharaja Sayajirao University of Baroda, Vadodara, India.*

Abstract

In the sphere of electrified transportation, the introduction of wireless charging systems for electric vehicle (EVs) is a significant development. The overall efficiency of EV wireless power transfer is greatly reduced when the transmitting and receiving power pads are loosely aligned. This paper presents mathematical model of square coil. The FEA model is prepared based on this mathematical model. Square power pad coil design is proposed from the results of FEA model. The effectiveness of wireless power transfer by square power pad coils numerous vertical, horizontal misalignment is analytical, and graphical (both 2D and 3D) presented. The detailed simulation and analysis have been carried out using industry standard ANSYS Electronic desktop software tool. The proposed design provides excellent wireless power transfer capability and reduced power losses with overall increased efficiency.

Keywords: Electric Vehicle, EV, Finite Element Analysis, Power Transfer Efficiency, Wireless Charging System, ANSYS.

Nomenclature

k	Coupling co-efficient
M	Mutual Inductance (Henry)
B	flux density
C	further nomenclature continues down the page inside the text box

Greek symbols

φ_n	Flux of nth region

1. Introduction:

An EV wireless charging system includes two components: vehicle assembly and ground assembly [1]-[2]. Each portion must have pads. EV wireless charging power pads are available in circular, double D (DD) and double D quadrature (DDQ) power pads in the research [9]–[11]. However, the most useful configuration is square pad. In DDQ power pads, the existing DD power pad is combined with a quadrature pad to produce a three compared to a square power pad, resulting in a times bigger power zone and improved performance at a variety of off-centre situations [7].

This paper has outlined an analytical method for calculating the mutual inductance between two coils. A thorough examination of all potential angular and lateral misalignments with respect to the horizontal and vertical versions is simulated. The geometry of square coil has been chosen here to examine the coils' alignment issues. The square coil configuration, simplifying difficult mathematical computations. A 3-D finite element analysis (FEA) is used to compare the results of the analytical model. Fig.1 shows the primary basic pieces for computing MI.

1.1. Analytical modelling of square coil

Modelling of Mutual Inductance: The coils' circuit topology has transmitting and receiving coils and is represented by an analogous circuit that resembles an inductively coupled transformer, such as the one in Fig. 1. Imagine that the transmitting and receiving coils are placed in close proximity to one another, as shown in the image. When electricity flows through the transmitting coil, it creates a magnetic flux that connects the receiving coil in part [3][5]. Now, the coil's mutual inductance (MI) is displayed and determined using

$$MI = \lambda_{12} / I$$

* Dilip R Dobariya
E-mail address: drdobariya@vgecg.ac.in

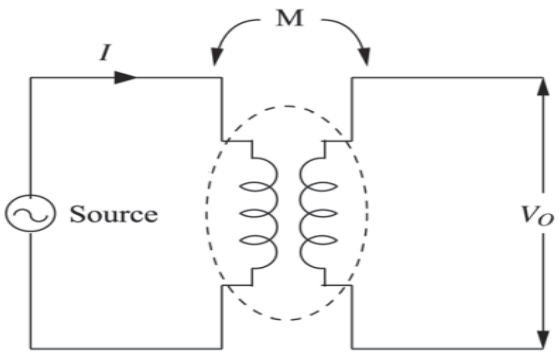

Fig.1. circuit topology of transmitting and receiving coil

The entire flux distribution can be found using the integration method of considering the whole coil as small coil of single turns [14]. The method can be used by using a tiny part of one turn of the entire coil. The flux linked by the tiny part can be considered for the calculation of whole coil and the mutual flux linked is estimated [12][8]. By repeating the process and more iteration, total flux linked with receiving coil can be found out. The sum of the flux linked in each little grid for all of the transmitting coils turns yields the total flux linked in the coil itself [7]. The maximum summation is determined by the quantity of tiny areas produced during a single OC turn. λ_{12} can be calculate by considering the flux (φ_n) of all small regions (nth) of a single turn of the coil.

$$\lambda_{12} = \sum \varphi_n \tag{1}$$

φ_n for each tiny portion can be calculated using following equations and it depends on the central magnetic field $\overrightarrow{B_c}$, area of tiny region (An) and the normal vector $\overrightarrow{A_n}$ [9].

$$\varphi_n = \overrightarrow{B_c}.(A_n.\vec{A}_n) \tag{2}$$

The magnetic field of the four sides of the square tiny coils can be found from Bio-Savart law, the magnetic field at any point in the space due to straight current carrying conductor is

$$\overrightarrow{B_n} = \int \frac{\mu_0 I \overrightarrow{d_s} X \hat{R}}{} \tag{3}$$

Here, $\hat{R}$ is the unit vector and started from $\overrightarrow{d_s}$ the current carrying conductor.

$$\varphi_1 = \sum^4 \frac{\mu_0}{} \int \frac{I\overrightarrow{d_s} X \widehat{R_1}}{}.(A_1.\widehat{A_1}) \tag{2}$$

And the total linked flux for entire turn can be found by

$$\varphi_m = \sum_{k=1}^{P} \sum(\varphi_1 + \varphi_2 \ldots + \varphi_n) \tag{5}$$

This procedure can be repeated to calculate λ12 for the entire coil using following equation.

$$\lambda_{12} = \sum_{m-1}^{Q} \varphi_m \tag{6}$$

1.2. Graphical modelling of square coil

The design obtain from the calculations are further used for the validation using FEA model in Fig.2. ANSYS Electronics desktop 2018.2 is used for the validation of the design. Both the coils are having same 21 turns and are excited with same current of 10 Ampere. The geometry for the coils is selected to be square.

Fig. 3 and Table:1 illustrates how the coupling coefficient varies for power pads with vertical and horizontal displacements varying from 5 to 200 mm between the coils. The value of the coupling coefficient represents the how both coils are magnetically coupled. For EV wireless charging systems, a stronger connection between the transmitting and receiving sides of power pads is indicated by a greater coupling coefficient.

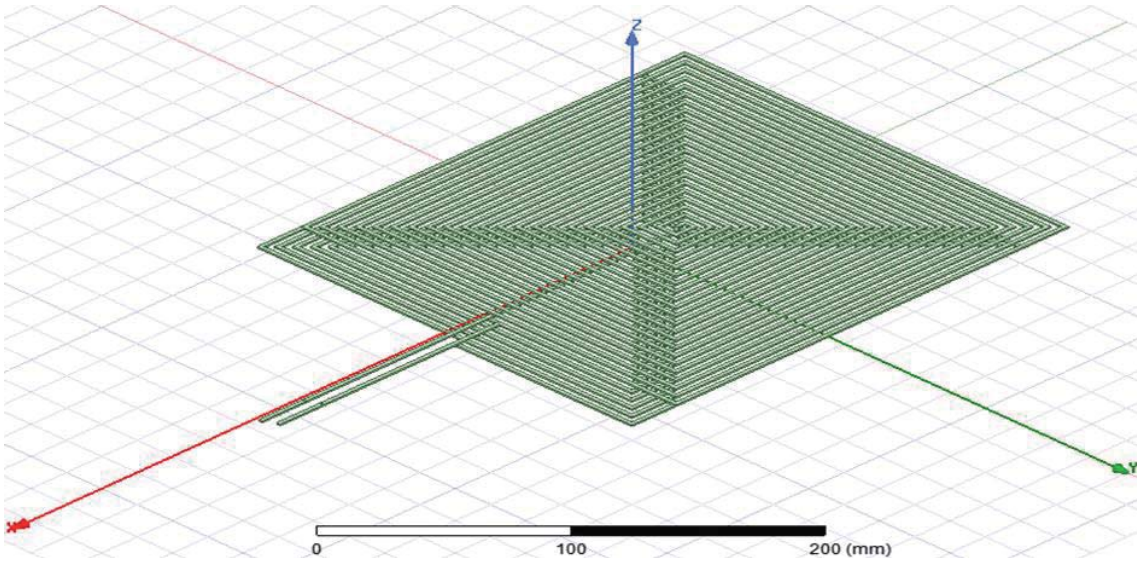

Fig.2. design model of transmitting and receiving coil in ANSYS Electronics Desktop

Table 1. Variation of coupling co-efficient with YDist and ZDist

	Coupling Co-efficient at various Z Distance							
YDist [mm]	25mm	50mm	75mm	100mm	125mm	150mm	175mm	200mm
-100	0.123609	0.103784	0.082828	0.063273	0.048624	0.037631	0.029364	0.023243
-92	0.163341	0.128562	0.096988	0.072424	0.054504	0.041871	0.031885	0.024911
-83	0.20479	0.154593	0.112765	0.081772	0.060273	0.045148	0.034416	0.026572
-75	0.247819	0.177923	0.127134	0.09113	0.065955	0.048756	0.036635	0.028159
-67	0.291874	0.205118	0.141735	0.099414	0.071271	0.052179	0.038915	0.02955
-58	0.337873	0.227476	0.155901	0.108019	0.076317	0.055318	0.040827	0.030889
-50	0.379372	0.250629	0.168446	0.115549	0.081849	0.058021	0.042673	0.031961
-42	0.42021	0.271433	0.179844	0.122056	0.084868	0.060491	0.044104	0.032921
-33	0.455774	0.290773	0.190279	0.128059	0.088408	0.062576	0.045405	0.033758
-25	0.487674	0.305897	0.198174	0.132582	0.091294	0.0642	0.046389	0.034296
-17	0.511836	0.318359	0.204634	0.135615	0.093934	0.065347	0.047049	0.034669
-8	0.526637	0.32501	0.206901	0.137831	0.094186	0.065719	0.047774	0.034721
0	0.533543	0.325397	0.208718	0.138058	0.093905	0.065737	0.047246	0.034553
8	0.527062	0.323159	0.208047	0.137651	0.094928	0.065749	0.047158	0.03471
17	0.511419	0.315997	0.203565	0.135648	0.092942	0.065176	0.0471	0.034676
25	0.486144	0.304109	0.198434	0.132788	0.090834	0.064072	0.046432	0.034332
33	0.456239	0.289391	0.189377	0.127824	0.088427	0.062363	0.045361	0.033702
42	0.41879	0.273915	0.17976	0.121704	0.084703	0.060561	0.044142	0.032875
50	0.380113	0.249825	0.167945	0.112435	0.080683	0.058006	0.042487	0.031923
58	0.33565	0.228063	0.155215	0.107775	0.076038	0.055226	0.040716	0.030747
67	0.290606	0.201959	0.14109	0.099148	0.070932	0.051968	0.038636	0.029462
75	0.247074	0.179236	0.126754	0.090217	0.065673	0.048493	0.036513	0.027993
83	0.204715	0.151502	0.111651	0.081245	0.060187	0.045006	0.034275	0.026445
92	0.163159	0.127622	0.096015	0.072214	0.054318	0.041683	0.031746	0.024885
100	0.123524	0.103333	0.007836	0.062909	0.048378	0.037404	0.029276	0.023183

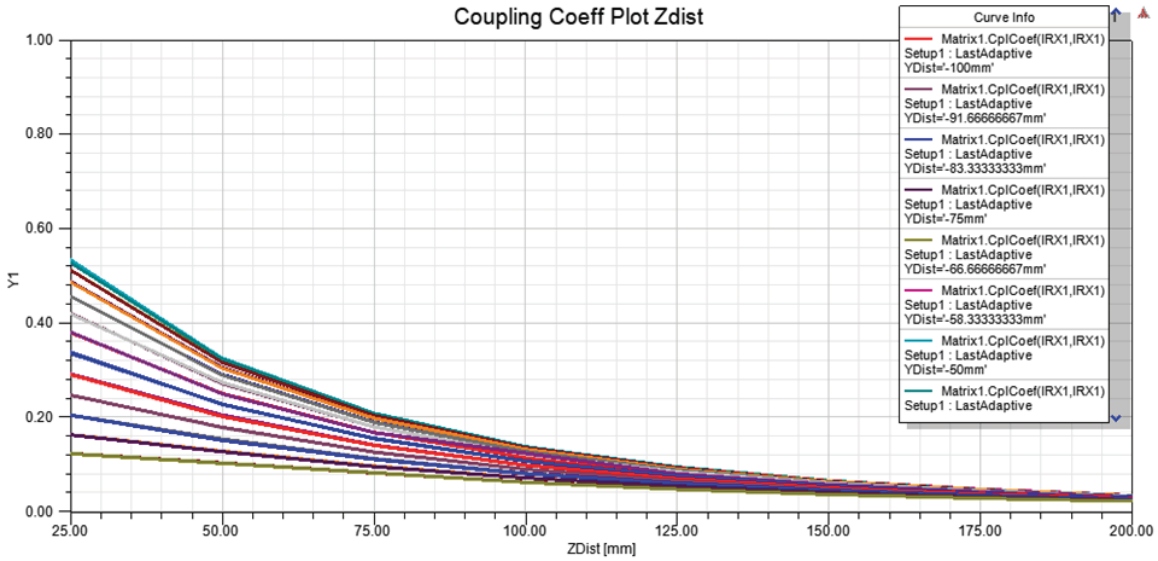

Fig.3. Variation of coupling co-efficient with ZDist

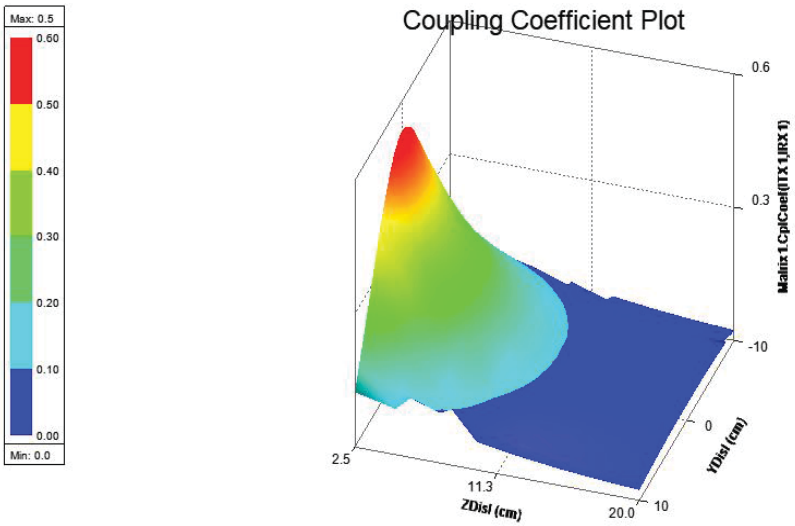

Fig.4. 3D plot showing variation of coupling co-efficient v/s YDist and v/s ZDist

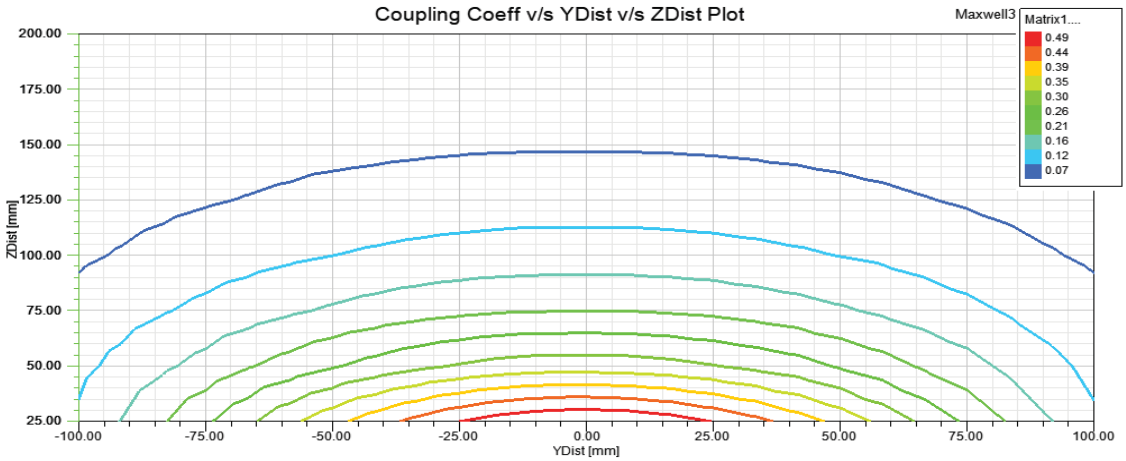

Fig.5. 2D plot of variation between coupling co-efficient, YDist and ZDist

Table 2. Variation of mutual inductance with YDist and ZDist

YDist [mm]	Mutual Inductance between transmitting and receiving coils (micro Henrry) Z Distance							
	25mm	50mm	75mm	100mm	125mm	150mm	175mm	200mm
-100	5.694506	4.82085	3.853374	2.934254	2.257223	1.747516	1.36422	1.073571
-92	7.52512	5.954284	4.49267	3.370942	2.530338	1.919726	1.480027	1.152238
-83	9.450005	7.097382	5.254859	3.786152	2.792646	2.093511	1.590893	1.227977
-75	11.46181	8.293882	5.932914	4.204504	3.056543	2.260453	1.701514	1.299325
-67	13.51455	9.449528	6.620632	4.614769	3.310973	2.421877	1.798602	1.366073
-58	15.54951	10.60778	7.261702	5.016178	3.544259	2.565139	1.899584	1.426029
-50	17.52699	11.6876	7.863091	5.355861	3.754386	2.697868	1.979528	1.479564
-42	19.39833	12.66704	8.397571	5.671417	3.943539	2.811422	2.047293	1.523864
-33	21.05912	13.51692	8.883294	5.938155	4.100783	2.903507	2.106082	1.559933
-25	22.48589	14.22152	9.220868	6.150366	4.22248	2.979989	2.148838	1.586089
-17	23.59237	14.72352	9.47682	6.30527	4.307741	3.025079	2.183057	1.601953
-8	24.28877	15.05203	9.668884	6.391889	4.355461	3.050577	2.187994	1.606396
0	24.52172	15.14355	9.724662	6.433312	4.363421	3.049385	2.187159	1.600264
8	24.26528	15.04974	9.684682	6.39002	4.353572	3.048862	2.189167	1.605504
17	23.56931	14.73533	9.495355	6.301591	4.305236	3.023066	2.183961	1.600202
25	22.45484	14.19945	9.211587	6.139601	4.219695	2.974492	2.148631	1.584873
33	21.02772	13.49904	8.842473	5.927847	4.091169	2.899665	2.105822	1.557288
42	19.33388	12.62267	8.390842	5.660986	3.934494	2.80137	2.044177	1.520897
50	17.47153	11.6452	7.820083	5.433432	3.747707	2.688938	1.971035	1.476292
58	15.48508	10.55289	7.245118	4.99881	3.533436	2.554739	1.889034	1.421859
67	13.43192	9.429085	6.583765	4.612446	3.300072	2.408715	1.797101	1.361425
75	11.38405	8.230991	5.906688	4.184624	3.042477	2.251271	1.688767	1.294435
83	9.376355	7.066922	5.208748	3.780467	2.779693	2.083816	1.586199	1.222637
92	7.440745	5.912258	4.462214	3.337293	2.510786	1.909638	1.47418	1.146493
100	5.624982	4.810278	3.657842	2.914367	2.243284	1.730842	1.353896	1.067338

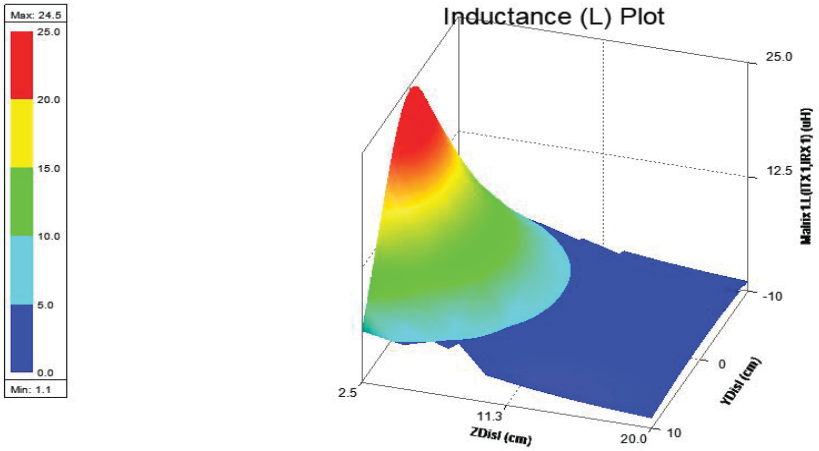

Fig.6. 3D plot of variation of mutual inductance, YDist & ZDist

After careful observation of Fig.6, we can say that mutual inductance between the two power pads is having larger values at the centres. As we are moving away from the centre in both the horizontal and planner directions, mutual inductance decreases.

2. Conclusion

An analytical technique based on the Biot-Savart law has been introduced in this study for calculating the MI between two air core square coils. MI is determined using a model of a spiral square coil. ANSYS Electronics Desktop has been used to make 3D models for power pads that are based on the SAE J2954 recommended physical dimensions and analysed for several misalignment scenarios and their variations. The horizontal and lateral misalignment of both the coils is studied and results presented in tabular as well as graphical (2D & 3D) forms. It has been found that when the distance between the coils increases, the coupling and MI between them decrease. The results of the analysis and FEA are in excellent agreement, and the result has an error of less than 10%.

References

1. Yui Hou,Yuan Jhou, Jian Wu, Huihui Song, Yanbin Qu, “A New Type of Curved Coupling Coil for Wireless Power Transmission,”22nd International Conference on Electrical Machines and Systems (ICEMS), pp. 19-25, Aug. 2019.
2. Tasnime Bouanou, Hassan El Fadil, Abdellah Lassioui,“Analysis and Design of Circular Coil Transformer in a Wireless Power Transfer System for Electric Vehicle Charging Application,” Proc IEEE 4th International Conference on Electrical and Information Technologies ICEIT’2020, 13-17 June, 2020.
3. Linlin Gao, Xingming Fan, Chao Wang, Yuanming Tan, Xin Zhang, “Coil Design of EVs Wireless Charging System Based on MCR-WPT,” 2018 11th International Symposium on Computational Intelligence and Design, pp. 169-172, 2018.
4. Maryam Salama Mohamed, Mohamed Abdul Raouf Shafei, Doaa Khalil Ibrahim, Ahmed Ali Mansour, “Coils Design and Parallel Resonant H-bridge Inverter for Inductive Power Transfer of Low-power portable devices,” 21st International Middle East Power Systems Conference (MEPCON), Tanta University, Egypt, pp.621-626, June, 2019.
5. K. Aditya and S. S. Williamson, "Comparative study of Series-Series and Series-Parallel Compensation Topologies for Electric Vehicle Charging," IEEE 23rd International Symposium on Industrial Electronics (ISIE), Istanbul, 2014, pp. 426-430.
6. Sallan J., Villa J. L., Llombart A., ve Sanz J. F., “Optimal Design of ICPT Systems Applied to Electric Vehicle Battery Charge,” in IEEE Trans. on Industrial Electronics, vol. 56, no. 6, pp. 2140-2149, June 2009.
7. Wang C.S., Covic G. A., ve Stielau O. H., “General Stability Criterions for Zero Phase Angle Controlled Loosely Coupled Inductive Power Transfer Systems,” in Proc. IEEE Annual Conf. of the Industrial Electronics Society, Denver, CO, vol. 2, Nov. 2001, pp. 1049-1054.
8. Wang C. S., Covic G. A., ve Stielau O. H., ‘‘Power Transfer Capability and Bifurcation Phenomena of Loosely Coupled Inductive Power Transfer Systems,’’ IEEE Transaction on Industrial Electronics, vol.51, no. 1, pp. 148–157, Feb. 2004.
9. Society of Automotive Engineers SAE J1772-2001 electric vehicle conductive charge coupler[S]USA2001.
10. Zhang Xian, Yang Qingxin, Cui Yulong, et al. “Design Optimization and Verification on the Power Transmitting Coil in the High-Power Wireless Power Transmission System,” Transactions of China Electrotechnical Society, vol. 28, Oct. 2013, pp. 12-18.
11. Cove S R Ordonez M Shafiei N et al. Improving Wireless Power Transfer Efficiency Using Hollow Windings with Track-Width Ratio[J]. IEEE Transactions on Power Electronics, 2015.
12. Meng W Jing F Yanyan S et al. Demagnetization Weakening and Magnetic Field Concentration with Ferrite Core Characterization for Efficient Wireless Power Transfer. IEEE Transactions on Industrial Electronics, 2018,66(3):1842-1851.
13. Ha-Van N, Seo C. Analytical and Experimental Investigations of Omnidirectional Wireless Power Transfer using a Cubic Transmitter. IEEE Transactions on Industrial Electronics, 2017:1-1.
14. M. Budhia, J.T. Boys, G.A. Covic, and C.–Y. Huang, “Development of a Single-Sided Flux Magnetic Coupler for Electric Vehicle IPT Charging Systems,” IEEE Transactions on Industrial Electronics, vol. 60. No. 1, pp. 318-328, January 2013, DOI: 10.1109/ IE.2011.2179274.
15. S. Chopra and P. Bauer, “Driving Range Extension of EV with On Road Contactless Power Transfer – a case study,” IEEE Trans. Ind. Electron., vol. 60, no. 1, pp. 329–338, Jan. 2013, DOI: 10.1109/ TIE.2011.2182015.
16. G.A. Covic and J.T. Boys, “Modern Trends in Inductive Power Transfer for Transportation Applications,” IEEE J. Emerging Sel. Topics Power Electron., vol. 1, no. 1, pp. 28–41, Mar. 2013, DOI:10.1109/JESTPE. 2013. 2264473.
17. N.Y. Kim, K. Y. Kim, J. Choi, and C.-W. Kim, “Adaptive Frequency with Power-Level Tracking System for Efficient Magnetic Resonance Wireless Power Transfer,” Electronics Letters, vol. 48, no. 8, pp. 452454, April 2012.

18. J.M. Miller, C.P. White, O.C. Onar, and P.M. Ryan, "Grid Side Regulation of Wireless Power Charging for Plug-in Electric Vehicles," in Proc., IEEE Energy Conversion Congress and Exposition (ECCE'12), pp. 261-268, September 2012, Raleigh, NC, DOI:10.1109/ECCE.2012. 6342814.
19. Zhijie Feng, Han Peng, Yong Chen "A Dual Resonance Electromagnetic Vibration Energy Harvester for Wide Harvested Frequency Range with Enhanced Output Power," in Proc., IEEE Energy Conversion Congress and Exposition (ECCE'12), pp. 261-268, September 2012, Raleigh, NC, DOI:10.1109/ECCE.2012. 6342814.